Received: 29 December 2017 | Revised: 29 January 2018 | Accepted: 1 February 2018

DOI: 10.1111/cas.13526

ORIGINAL ARTICLE

WILEY Cancer Science

Impact of novel oncogenic pathways regulated by antitumor *miR-451a* in renal cell carcinoma

Yasutaka Yamada[1,2] | Takayuki Arai[1,2] | Sho Sugawara[1,2] | Atsushi Okato[1,2] | Mayuko Kato[2] | Satoko Kojima[3] | Kazuto Yamazaki[4] | Yukio Naya[3] | Tomohiko Ichikawa[2] | Naohiko Seki[1]

[1]Department of Functional Genomics, Chiba University Graduate School of Medicine, Chiba, Japan

[2]Department of Urology, Chiba University Graduate School of Medicine, Chiba, Japan

[3]Department of Urology, Teikyo University Chiba Medical Center, Ichihara, Japan

[4]Department of Pathology, Teikyo University Chiba Medical Center, Ichihara, Japan

Correspondence
Naohiko Seki, Department of Functional Genomics, Chiba University Graduate School of Medicine, Chiba, Japan.
Email: naoseki@faculty.chiba-u.jp

Funding information
Japan Society for the Promotion of Science (16K20125, 17K11160, 16H05462, and 15K10801).

Recent analyses of our microRNA (miRNA) expression signatures obtained from several types of cancer have provided novel information on their molecular pathology. In renal cell carcinoma (RCC), expression of microRNA-451a (*miR-451a*) was significantly downregulated in patient specimens and low expression of *miR-451a* was significantly associated with poor prognosis of RCC patients ($P = .00305$) based on data in The Cancer Genome Atlas. The aims of the present study were to investigate the antitumor roles of *miR-451a* and to identify novel oncogenic networks it regulated in RCC cells. Ectopic expression of *miR-451a* significantly inhibited cancer cell migration and invasion by RCC cell lines, suggesting that *miR-451a* had antitumor roles. To identify oncogenes regulated by *miR-451a* in RCC cells, we analyzed genome-wide gene expression data and examined information in in silico databases. A total of 16 oncogenes and were found to be possible targets of *miR-451a* regulation. Interestingly, high expression of 9 genes (*PMM2*, *CRELD2*, *CLEC2D*, *SPC25*, *BST2*, *EVL*, *TBX15*, *DPYSL3*, and *NAMPT*) was significantly associated with poor prognosis. In this study, we focused on phosphomannomutase 2 (*PMM2*), which was the most strongly associated with prognosis. Overexpression of *PMM2* was detected in clinical specimens and Spearman's rank test indicated a negative correlation between the expression levels of *miR-451a* and *PMM2* ($P = .0409$). Knockdown of *PMM2* in RCC cells inhibited cancer cell migration and invasion, indicating overexpression of *PMM2* could promote malignancy. Analytic strategies based on antitumor miRNAs is an effective tool for identification of novel pathways of cancer.

KEYWORDS
antitumor, microRNA, *miR-451a*, *PMM2*, renal cell carcinoma

1 | INTRODUCTION

Renal cell carcinoma (RCC) is the most common form of kidney cancer and is diagnosed in more than 350 000 patients worldwide, making it the seventh most common site for tumors.[1] Although patients with stage I RCC had a 5-years survival rate above 90%, those with advanced RCC had a 5-years survival rate of only 23%.[2] In fact, 25%-30% of patients have metastasis at the time of diagnosis.[3] Furthermore, distant metastasis and recurrence are found even when surgical resection is carried out for localized RCC, cases that are associated with poor prognosis. Recently, molecular targeted therapy and immunotherapy have been used for patients with metastatic or

This is an open access article under the terms of the Creative Commons Attribution-NonCommercial-NoDerivs License, which permits use and distribution in any medium, provided the original work is properly cited, the use is non-commercial and no modifications or adaptations are made.
© 2018 The Authors. *Cancer Science* published by John Wiley & Sons Australia, Ltd on behalf of Japanese Cancer Association.

recurrent RCC. However, the therapeutic benefits are limited, and RCC is generally insensitive to radiation and chemotherapy. Thus, development of novel therapeutic strategies is needed.[2] We believe that novel genomic approaches are required to elucidate the underlying molecular mechanism of metastatic RCC.

MicroRNA (miRNA) is a single-stranded low molecular RNA of 19-22 bases that possesses important functions. For example, miRNA regulates the expression of target genes by inhibiting translation and/or accelerates the degradation of functional RNAs (protein coding/non-protein coding genes).[4,5] In human cells, a single miRNA can regulate many different protein-coding or non-coding mRNAs and a single mRNA can be regulated by several different miRNAs.[6] Thus, aberrant expression of miRNA could disrupt regulated RNA networks in cancer cells. Therefore, it is important to elucidate the aberrant expression of miRNAs in each type of cancer to better understand the molecular mechanism of cancer pathogenesis.[4,7,8]

We previously identified antitumor miRNAs that regulated novel oncogenic pathways based on miRNA expression signatures.[9-12] Downregulation of *miR-451a* was detected by our studies of miRNA signatures and several types of cancers.[12-18] Moreover, a large cohort analysis using The Cancer Genome Atlas (TCGA) database (https://cancergenome.nih.gov/) showed that low expression of *miR-451a* was associated with poor survival of patients with RCC. The antitumor role of *miR-451a* in RCC has been reported;[19] however, the molecular pathways regulated by *miR-451a* have not been fully elucidated. MicroRNA biogenesis is unique, in that a single miRNA can target a vast number of RNAs in cells. Continuous analyses of antitumor miRNA-regulated molecular pathways are essential for understanding RCC pathogenesis. Here, we aimed to investigate novel oncogenic pathways regulated by antitumor *miR-451a* in RCC cells and involving in RCC pathogenesis.

2 | MATERIALS AND METHODS

2.1 | Patients, cancer tissue collection, cell lines, and cell culture

We postoperatively collected cancerous and normal tissues from 15 RCC patients at Chiba University Hospital (Chiba, Japan) between 2012 and 2015. Clinicopathological characteristics of the 15 patients are listed in Table 1. Tumor stages were determined by the General Rule for Clinical and Pathological Studies on Renal Cell Carcinoma based on the AJCC-UICC TNM classification. All patients gave signed, informed consent for the use of the tissues for research purposes.

We used 2 human RCC cell lines (786-O and A498) obtained from ATCC (Manassas, VA, USA) as previously described.[20-25] These cell lines were maintained in RPMI-1640 with 10% FBS (HyClone, Logan, UT, USA).

2.2 | Transfections with mature miRNA, siRNA, or plasmid vectors

We used the following mature miRNA species in these experiments: mature miRNA and pre-miR miRNA precursors (*has-miR-451a*; P/N: AM17100; Applied Biosystems, Foster City, CA, USA). The following siRNAs were used: Stealth Select RNAi siRNA, si-*PMM2* (HSS108164 and HSS108165; Invitrogen, Carlsbad, CA, USA), and negative control miRNA/siRNA (P/N: AM17111; Applied Biosystems). *PMM2* plasmid vectors were designed and provided by OriGene (cat. no. RC203472; Rockville, MD, USA). MicroRNAs and siRNAs were incubated with Opti-MEM (Invitrogen) and Lipofectamine RNAiMax transfection reagent (Invitrogen), as previously described.[22,26] Plasmid vectors were incubated with Opti-MEM and

TABLE 1 Clinical features of 15 patients with clear cell renal cell carcinoma

Patient no.	Age, years	Gender	Grade	pT	INF	v	ly	eg or ig	fc	im	rc	rp	s
1	71	F	G2	T1a	a	0	0	eg	1	0	0	0	0
2	74	M	G1 > G2	T1a	a	0	0	eg	1	0	0	0	0
3	59	M	G3 > G2	T1b	a	0	0	eg	1	0	0	0	0
4	52	M	G2 > G3 > G1	T1a	a	0	0	eg	1	0	0	0	0
5	64	M	G2 > G3	T1b	a	0	0	eg	1	1	0	0	0
6	67	M	G2 > G3 > G1	T3a	b	1	0	ig	0	1	1	0	0
7	67	M	G2 > G3 > G1	T3a	b	1	0	ig	1	0	0	0	0
8	59	M	G3 > G2	T3a	b	1	0	ig	0	0	0	0	0
9	73	M	G1 > G3	T2a	a	0	1	eg	1	0	0	0	0
10	77	M	G1 > G2	T1b	a	0	0	eg	1	0	0	0	0
11	77	M	G2 > G1	T3a	a	1	0	eg	1	0	0	0	0
12	51	M	G2 > G1	T1	a	0	0	eg	0	0	0	0	0
13	78	M	G2 > G1 > G3	T1b	b	0	0	eg	1	0	0	0	0
14	57	M	G1 > G2	T1a	a	0	0	eg	1	0	0	0	0
15	54	M	G2 > G1	T3a	a	0	0	eg	0	0	1	0	0

eg, expansive growth; F, female; fc, capsular formation; ig, infiltrative growth; im, intrarenal metastasis; INF, infiltration; ly, lymph node; M, male; rc, renal capsule invasion; rp, pelvis invasion; s, sinus invasion; v, vein.

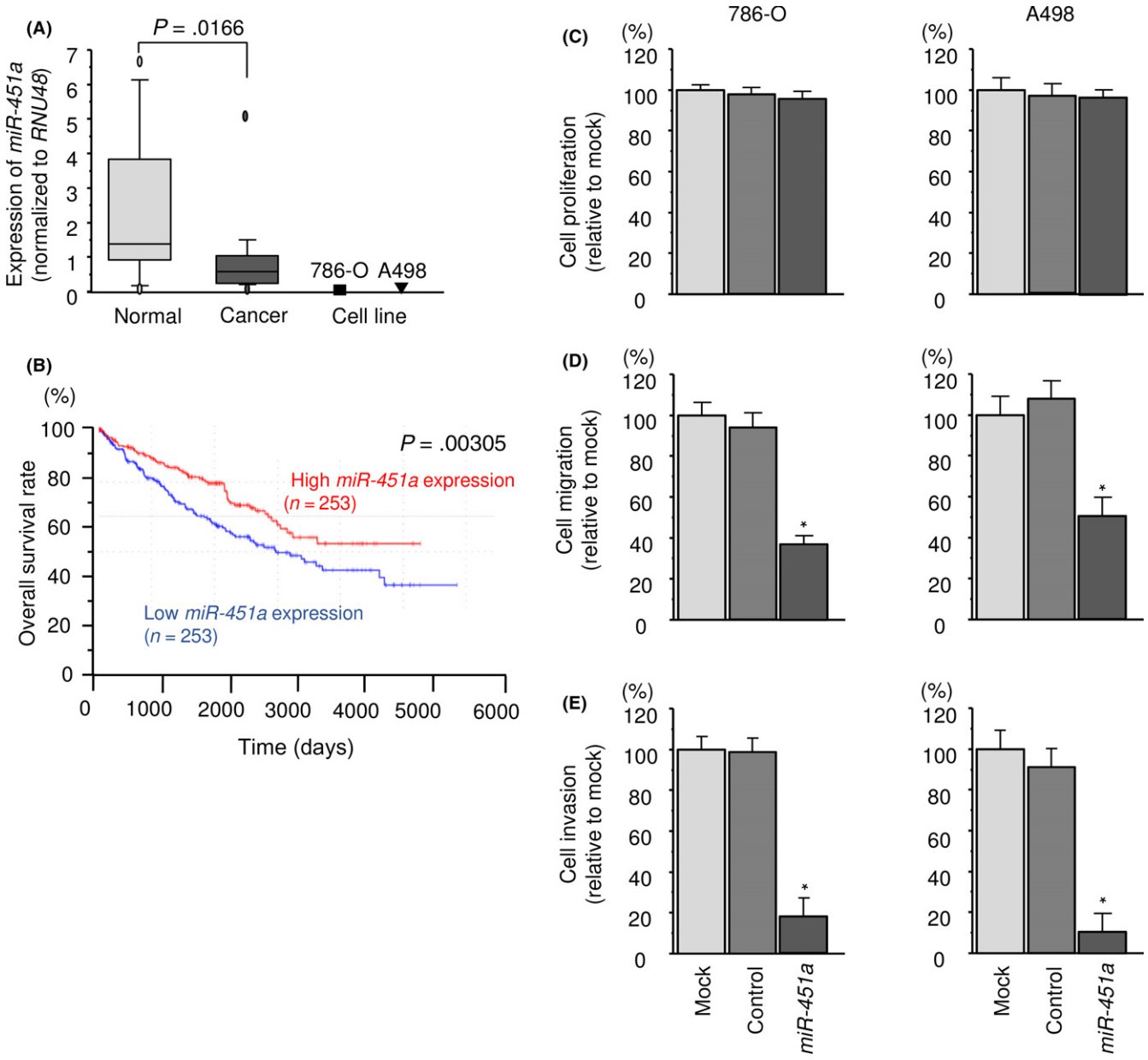

FIGURE 1 Antitumor functions of *miR-451a* in renal cell carcinoma. A, Expression levels of *miR-451a* in renal cell carcinoma clinical specimens and cell lines. *RNU48* was used as an internal control. B, Kaplan-Meier survival curves, as determined using data from The Cancer Genome Atlas database. C, Cell proliferation was determined by XTT assays 72 hours after transfection with *miR-451a*. D, Cell migration activity. E, Cell invasion activity was determined using Matrigel assays. *$P < .0001$

Lipofectamine 3000 reagent (Invitrogen) by forward transfection following the manufacturer's protocol.

2.3 | Quantitative real-time RT-PCR

Total RNA was extracted from human tissues and cell lines using TRIzol reagent (Invitrogen) according to the manufacturer's protocol, as we described previously.[20-25] The procedure for PCR quantification has been outlined. Expression levels of *miR-451a* (assay ID:001141; Applied Biosystems) were analyzed by TaqMan quantitative real-time RT-PCR (qRT-PCR) (TaqMan MicroRNA Assay; Applied Biosystems) and normalized to the expression of *RNU48* (assay ID: 001006; Applied Biosystems). TaqMan probes and primers for *PMM2* (P/N: Hs00756707_m1; Applied Biosystems), *GAPDH* (internal control; P/N: Hs02758991_m1; Applied Biosystems), and *GUSB* (internal control; P/N: Hs00939627_ml; Applied Biosystems) were assay-on-demand gene expression products. The relative expression levels were calculated using the $2^{-\Delta\Delta CT}$ method.

2.4 | Cell proliferation, migration, and invasion assays

Cell proliferation, migration, and invasion assays have been described.[20-25]

2.5 | Identification of putative target genes regulated by *miR-451a* in RCC cells

To identify *miR-451a* target genes, we used in silico analyses and genome-wide gene expression analyses, as outlined previously.[20-25] We used the TargetScanHuman 7.0 (August 2015 release) (http://www.targetscan.org/), TCGA, and OncoLnc datasets (http://www.oncolnc.org/) to select and narrow down putative miRNA target genes.[27-29] An oligo microarray (Human Ge 60K; Agilent Technologies) was used for gene expression analysis. We deposited the microarray data into the Gene Expression Omnibus (GEO) database.

2.6 | Western blot analysis

Cells were collected 48 hours after transfection, and lysates were prepared. Immunoblotting was undertaken with rabbit anti-PMM2 antibodies (1:500 dilution, SAB2702078; Sigma-Aldrich, St. Louis, MO, USA). Anti-GAPDH antibodies (1:10 000, ab8245; Abcam) were used as an internal loading control. The procedures have been described.[20-25]

2.7 | Plasmid construction and dual luciferase reporter assays

The partial wild-type sequence of the *PMM2* 3′-UTR or that with deletion of the *miR-451a* putative target site was inserted between the *Sgf*I-*Pme*I restriction sites in the 3′-UTR of the *hRluc* gene in the psiCHECK-2 vector (C8021; Promega, Madison, WI, USA). The procedures were covered in earlier reports.[20-25]

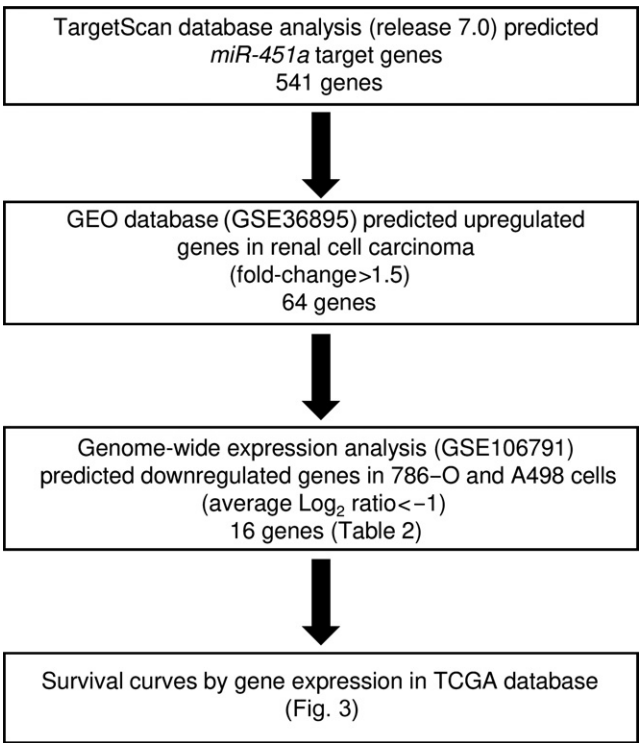

FIGURE 2 Flow chart illustrating the analytic strategy for *miR-451a* targets in renal cell carcinoma cells. A total of 541 genes were putative targets of *miR-451a* in the TargetScan database analysis (release 7.0). We selected 16 genes as putative targets of *miR-451a* in renal cell carcinoma cells. GEO, Gene Expression Omnibus; TCGA, The Cancer Genome Atlas

2.8 | Immunohistochemistry

We used a tissue microarray that was incubated overnight at 4°C with anti-PMM2 antibodies (1:100 dilution, SAB2702078; Sigma-Aldrich). The sliced slides were treated with biotinylated goat antibodies (Histofine SAB-PO kit; Nichirei, Tokyo, Japan). The procedures were described earlier.[20-25]

2.9 | Regulation of targets downstream of *PMM2* in RCC

We analyzed *PMM2*-regulated pathways in RCC cells. We analyzed gene expression using si-*PMM2*-transfected 786-O cells. Microarray data were used for expression profiling of si-*PMM2* transfectants. The microarray data were deposited into the GEO database (accession no. GSE107008).

2.10 | The Cancer Genome Atlas database analysis of RCC

To assess the clinical significance of miRNAs and their targeted genes, we used the RNA sequencing database in TCGA. The definition of high and low expression divided half of the clinical data population in the order of expression. Gene expression and clinical data were obtained from cBioportal and OncoLnc (data downloaded November 1, 2017).[27-29]

2.11 | Statistical analysis

Relationships between 2 groups and the numerical values obtained by qRT-PCR were analyzed by Mann-Whitney *U*-tests and paired *t* tests. Spearman's rank test was used to analyze the correlation between the expression levels of *miR-451a* and *PMM2*. Relationships among more than 3 variables and numerical values were analyzed with Bonferroni-adjusted Mann-Whitney *U*-tests. Survival analysis was carried out using the Kaplan-Meier method, log-rank tests, and multivariable Cox hazard regression analyses with JMP software (version 13; SAS Institute, Cary, NC, USA). Other statistical analyses were carried out using Expert StatView (version 5; SAS Institute).

3 | RESULTS

3.1 | Expression levels of *miR-451a* in RCC clinical specimens and cell lines

Expression levels of *miR-451a* were significantly downregulated in RCC tissues compared with those in non-cancerous tissues ($P = .0166$; Figure 1A). Furthermore, expression levels of *miR-451a* in 786-O and A498 cells were markedly downregulated (Figure 1A).

TABLE 2 Candidate target genes regulated by *miR-451a* in renal cell carcinoma cells

Gene symbol	Gene name	Conserved sites count	Poorly conserved sites count	GEO expression data fold-change (tumor/normal)	A498 *miR-451a* transfection (Log_2 ratio)	786-O *miR-451a* transfection (Log_2 ratio)	Average A498/786-O *miR-451a* transfection (Log_2 ratio)	Cytoband	TCGA data OS (*P*-value)
PMM2	Phosphomannomutase 2	1	0	1.580	−1.617	−1.020	−1.319	hs|16p13.2	.000000218
CRELD2	Cysteine-rich with EGF-like domains 2	0	1	1.656	−1.724	−2.256	−1.990	hs|22q13.33	.000000831
CLEC2D	C-type lectin domain family 2, member D	0	1	2.557	−1.014	−1.455	−1.235	hs|12p13.31	.00009140
SPC25	SPC25, NDC80 kinetochore complex component	0	1	3.213	−2.497	−2.321	−2.409	hs|2q31.1	.00009800
BST2	Bone marrow stromal cell antigen 2	0	1	2.061	−0.668	−1.723	−1.196	hs|19p13.11	.00015300
EVL	Enah/Vasp-like	0	1	1.896	−1.197	−1.510	−1.354	hs|14q32.2	.00125000
TBX15	T-box 15	0	1	4.118	−1.224	−1.618	−1.421	hs|1p12	.00193000
DPYSL3	Dihydropyrimidinase-like 3	0	1	2.326	−1.325	−1.344	−1.335	hs|5q32	.00389000
NAMPT	Nicotinamide phosphoribosyltransferase	0	1	2.174	−2.369	−0.534	−1.452	hs|7q22.3	.01380000
MEGF6	Multiple EGF-like-domains 6	0	1	2.112	−0.917	−1.811	−1.364	hs|1p36.32	.15100000
CRIP2	Cysteine-rich protein 2	0	1	1.590	−1.899	−1.593	−1.746	hs|14q32.33	.18800000
CAV1	Caveolin 1, caveolae protein, 22kda	0	1	6.729	−1.196	−2.144	−1.670	hs|7q31.2	.20100000
PSMB8	Proteasome (prosome, macropain) subunit, beta type, 8	1	0	2.682	−1.502	−1.906	−1.704	hs|6p21.32	.25500000
CDH11	Cadherin 11, type 2, OB-cadherin (osteoblast)	0	1	1.847	−0.791	−1.788	−1.290	hs|16q21	.42600000
EGLN3	Egl-9 family hypoxia-inducible factor 3	0	1	13.668	−0.740	−1.940	−1.340	hs|14q13.1	.68800000
SLC39A14	Solute carrier family 39 (zinc transporter), member 14	0	1	2.057	−1.391	−1.386	−1.389	hs|8p21.3	.83600000

GEO, Gene Expression Omnibus; OS, overall survival; TCGA, The Cancer Genome Atlas.

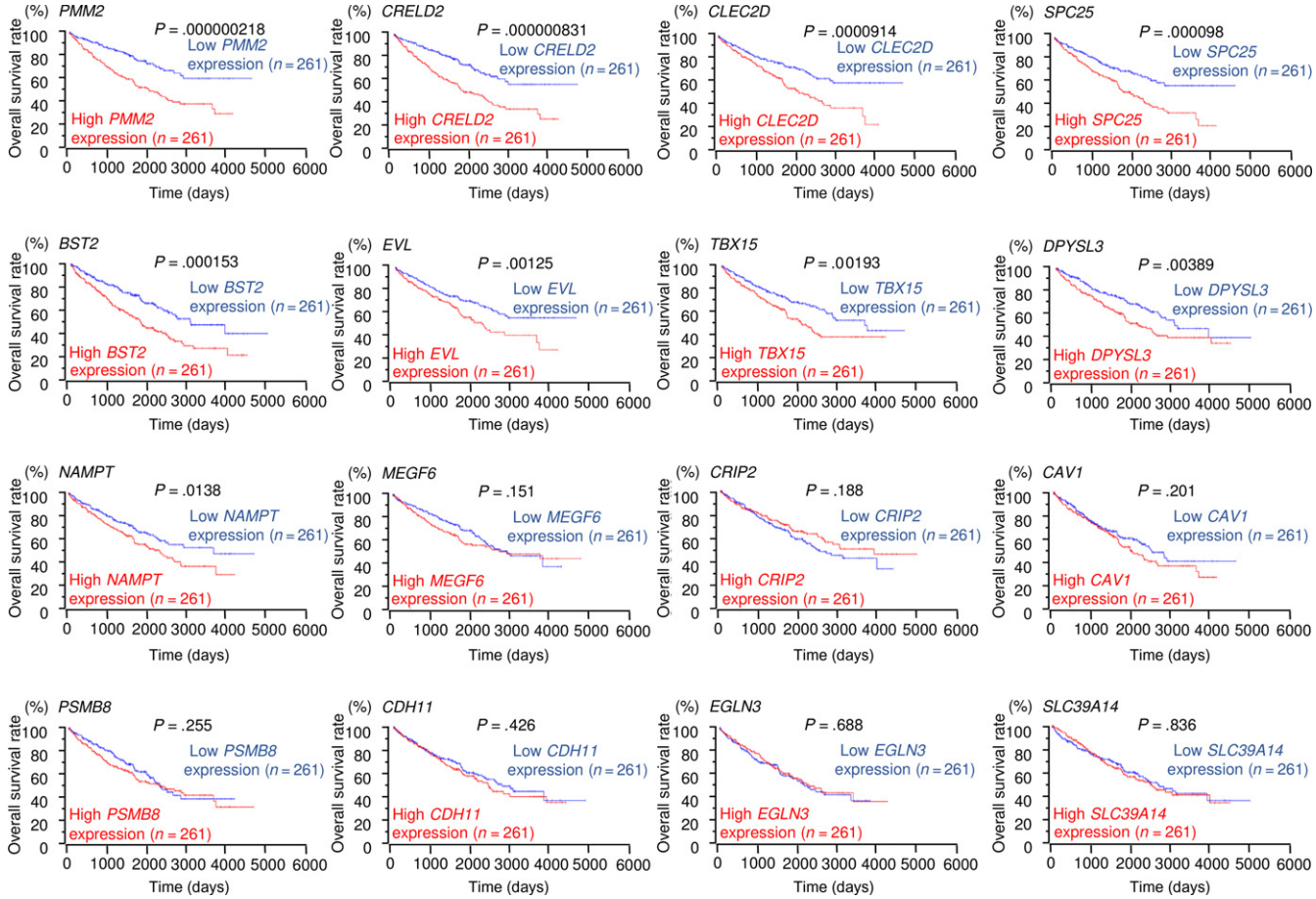

FIGURE 3 The Cancer Genome Atlas database analysis of putative targets of *miR-451a* in renal cell carcinoma. Kaplan-Meier plots of overall survival with log-rank tests for 16 genes with high and low expression from The Cancer Genome Atlas database

In the human genome, *miR-451a* has formed a miRNA cluster with other miRNAs (*miR-144-5p*, *miR-144-3p*, *miR-451b*, and *miR-4732*) on human chromosome 17q11.2 region (Figure S1). We also checked expression of these miRNAs in RCC clinical specimens. Expression levels of *miR-144-5p* and *miR-144-3p* were significantly downregulated in RCC tissues. On the contrary, it was revealed that the expression levels of *miR-451b* and *miR-4732* were extremely low in normal kidney and RCC tissues (Figure S1).

To investigate the molecular mechanisms of silencing of *miR-451a* in RCC cells, 786-O cells were treated with the demethylating agent 5-aza-2′-deoxycytidine. Expression of *miR-451a* was not dramatically elevated by 5-aza-2′-deoxycytidine treatment (Figure S1).

A large cohort analysis (n = 506) using data from TCGA database showed that low expression of *miR-451a* was associated with poor survival of patients with RCC ($P = .00305$; Figure 1B).

3.2 | Effects of ectopic expression of *miR-451a* in RCC cell lines

To investigate the antitumor functions of *miR-451a* in RCC cells, we applied to gain-of-function analyses in this study. Ectopic expression of *miR-451a* in RCC cell lines (786-O and A498) did not affect cell proliferation (Figure 1C). Cell migration and invasion activities were significantly inhibited in *miR-451a* transfectant cells compared with those in mock or miRNA-control transfectant cells (Figure 1D,E).

3.3 | Screening of candidate targets by *miR-451a* regulation in RCC cells

We undertook in silico and gene expression analyses to identify genes targeted by *miR-451a*. The strategy for selection of *miR-451a* target genes is shown in Figure 2. Using the TargetScanHuman 7.0 database, we identified 541 genes that had putative target sites for *miR-451a* in their 3′-UTRs. Among these genes, we identified 64 that showed increased expression levels in RCC tissues (fold-change >1.5) using the database (GEO database accession number: GSE36895).

Next, we identified 16 genes that were downregulated after transfection of 786-O and A498 cells with *miR-451a* (average $\log_2$ ratio < -1.0; Table 2). Next, using the OncoLnc database, we investigated whether the expression levels of the 16 candidate genes affected the prognosis of RCC patients. Kaplan-Meier survival curves revealed that high expression levels of 9 of the genes were

associated with poor prognosis in patients with RCC (Figure 3). Finally, we focused on *PMM2* because it showed the most evident difference in OncoLnc prognostic analysis ($P = .000000218$; Table 2, Figure 3) and there are few reports on cancer studies.

3.4 | *PMM2* directly regulated by *miR-451a* in RCC cells

Expression levels of *PMM2*/PMM2 were reduced by *miR-451a* transfection at mRNA and protein levels (Figure 4A,B).

Furthermore, we carried out luciferase reporter assays to elucidate whether *PMM2* mRNA had a functional target site for *miR-451a*. The TargetScan database predicted that *miR-451a* was bound at position 1127-1133 in the 3′-UTR of *PMM2* (Figure 4C). We used vectors encoding a partial wild-type sequence of the 3′-UTR of *PMM2* mRNA, including the predicted *miR-451a* target site, or a vector lacking the *miR-451a* target site. Luminescence intensity was significantly reduced by co-transfection with *miR-451a* and the vector carrying the wild-type 3′-UTR of *PMM2*. In contrast, luminescence intensity was not reduced when the target site of *miR-451a* was deleted from the vectors (Figure 4D).

3.5 | Effects of *PMM2* knockdown in RCC cell lines

To investigate the functional significance of *PMM2*, we carried out loss-of-function studies using transfection of si-*PMM2* into 786-O and A498 cells. First, we evaluated the knockdown efficiency of si-*PMM2* transfection, using 2 types of si-*PMM2* (si-*PMM2*_1 and si-*PMM2*_2). Using qRT-PCR and Western blot analyses, we confirmed that the expression levels of *PMM2* mRNA and protein were significantly reduced (Figure 5A,B). Furthermore, functional assays showed that si-*PMM2* transfection significantly inhibited cell proliferation, migration, and invasion in comparison with mock or siRNA-control transfected cells (Figure 5C-E).

3.6 | Expression of *PMM2*/PMM2 in RCC clinical specimens and cell lines

We used qRT-PCR to investigate the mRNA expression levels of *PMM2* in 15 pairs of RCC tissues, adjacent noncancerous tissues and RCC cell lines. Expression of *PMM2* was significantly upregulated in RCC tissues compared with that in normal tissues ($P = .0026$; Figure 6A) and also markedly upregulated in RCC cell lines.

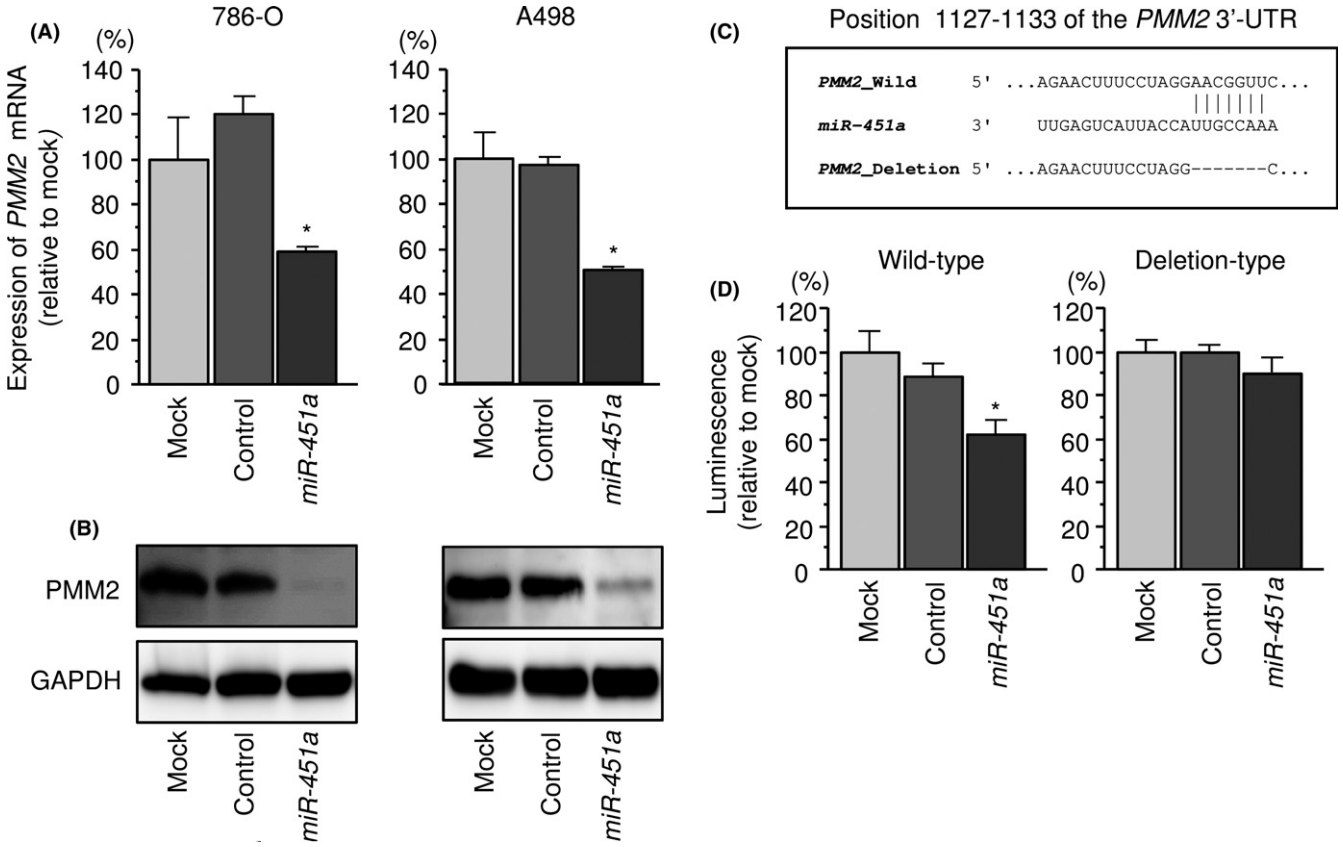

FIGURE 4 Regulation of *PMM2* expression by *miR-451a* in renal cell carcinoma cells. A, Expression levels of *PMM2* mRNA 48 hours after transfection of 10 nmol/L *miR-451a* into cell lines. *GUSB* was used as an internal control. *$P < .0001$. B, Protein expression of phosphomannomutase 2 (PMM2) 72 hours after transfection with *miR-451a*. GAPDH was used as a loading control. C, *miR-451a* binding sites in the 3′-UTR of *PMM2* mRNA. D, Dual luciferase reporter assays using vectors encoding putative *miR-451a* target sites (positions 1127-1133) in the *PMM2* 3′-UTR for both wild-type and deleted regions. Normalized data were calculated as the ratio of *Renilla*/firefly luciferase activities. *$P < .005$

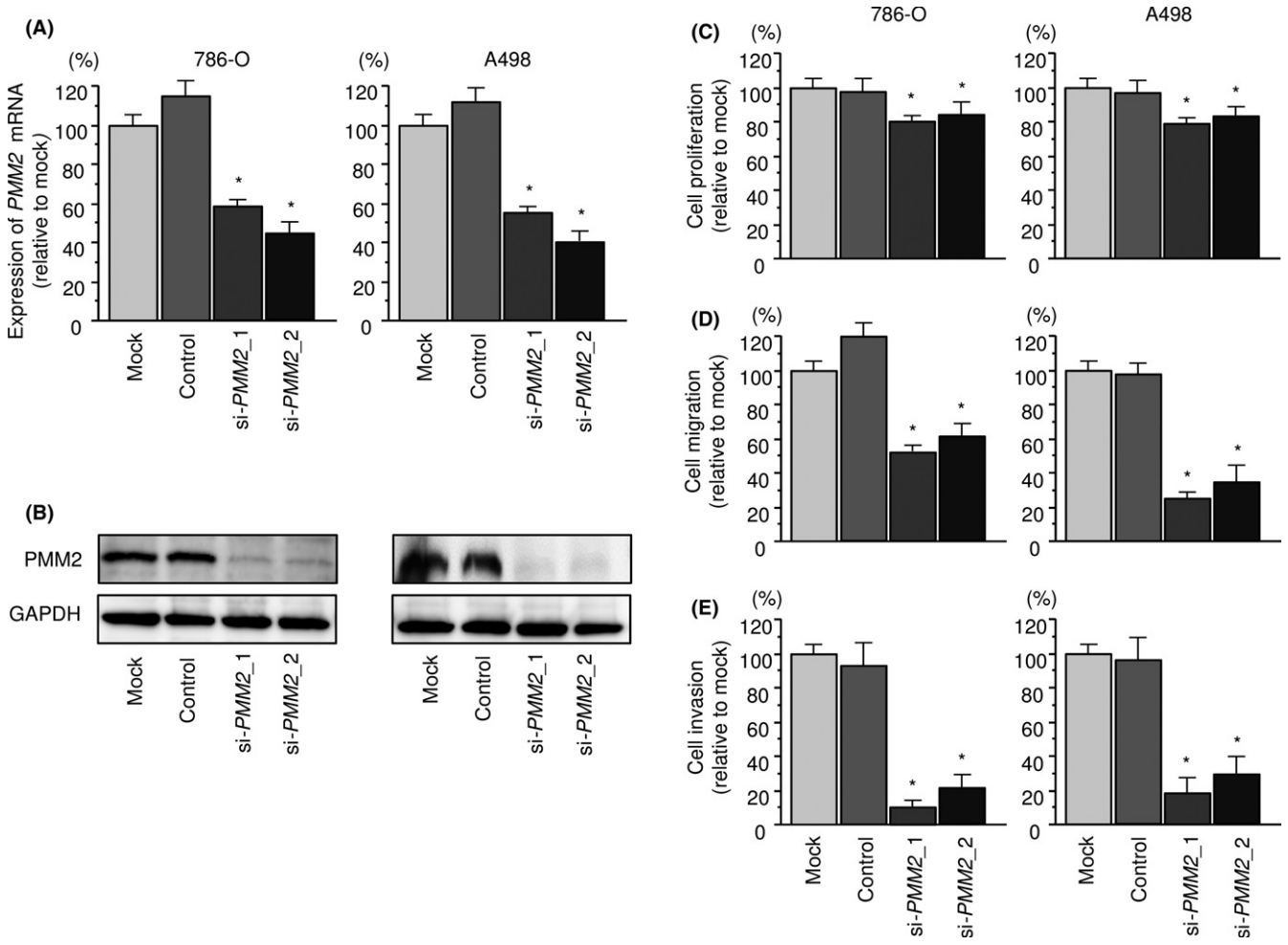

FIGURE 5 Effects of *PMM2* silencing in renal cell carcinoma cell lines. A, *PMM2* mRNA expression 48 hours after transfection with 10 nM si-*PMM2* into renal cell carcinoma cell lines. *GUSB* was used as an internal control. B, Phosphomannomutase 2 (PMM2) protein expression 72 h after transfection with si-*PMM2*. GAPDH was used as a loading control. C, Cell proliferation was determined with XTT assays 72 hours after transfection with 10 nM si-*PMM2*_1 or si-*PMM2*_2. D, Cell migration assessed by wound healing assays. E, Cell invasion activity was determined using a Matrigel system. *$P < .0001$

Furthermore, Spearman's rank test revealed a negative correlation between the expression levels of *miR-451a* and *PMM2* ($P = .0409$, $R = -.38$; Figure 6B).

Moreover, we carried out immunohistochemistry to analyze PMM2 protein expression in an RCC tissue microarray (cat. no. KD806; US Biomax, Rockville, MD, USA). Patient characteristics for samples used in the tissue microarray are as described in http://www.biomax.us/tissue-arrays/Kidney/KD806. The PMM2 protein was strongly expressed in several cancer lesions (Figure 6C).

3.7 | Effects of co-transfection of *PMM2*/*miR-451a* in 786-O cells

We undertook *PMM2* rescue studies in 786-O cells to elucidate whether the molecular pathway of *PMM2*/*miR-451a* was significant for the progression of RCC. Figure 7A shows the results of Western blot analysis of PMM2 protein expression. Functional assays showed that the migration and invasive abilities of RCC cells were significantly recovered by *PMM2* and *miR-451a* transfection compared with cells transfected with *miR-451a* alone (Figure 7C,D). These results suggested that *PMM2* had an important role in the aggressiveness of RCC.

3.8 | Downstream genes affected by silencing of *PMM2* in 786-O cells

We carried out genome-wide gene expression analyses by transfecting si-*PMM2* into 786-O cells to elucidate which genes were modulated by *PMM2* knockdown. We focused on genes that were significantly downregulated by transfection of both si-*PMM2*_1 and si-*PMM2*_2 (average $\log_2$ [si-*PMM2*/mock] < -1.0). Genes significantly downregulated by silencing of *PMM2* are listed in Table 3. Among these genes, high expression levels of *CD7*, *CCNE2*, *ASB2*, *RCN3*, *HSF1*, *PAQR4*, *CD37*, *SOX11*, *XAF1*, and *DEPDC1* were associated with poor prognosis in RCC patients based on TCGA database (Figure 8).

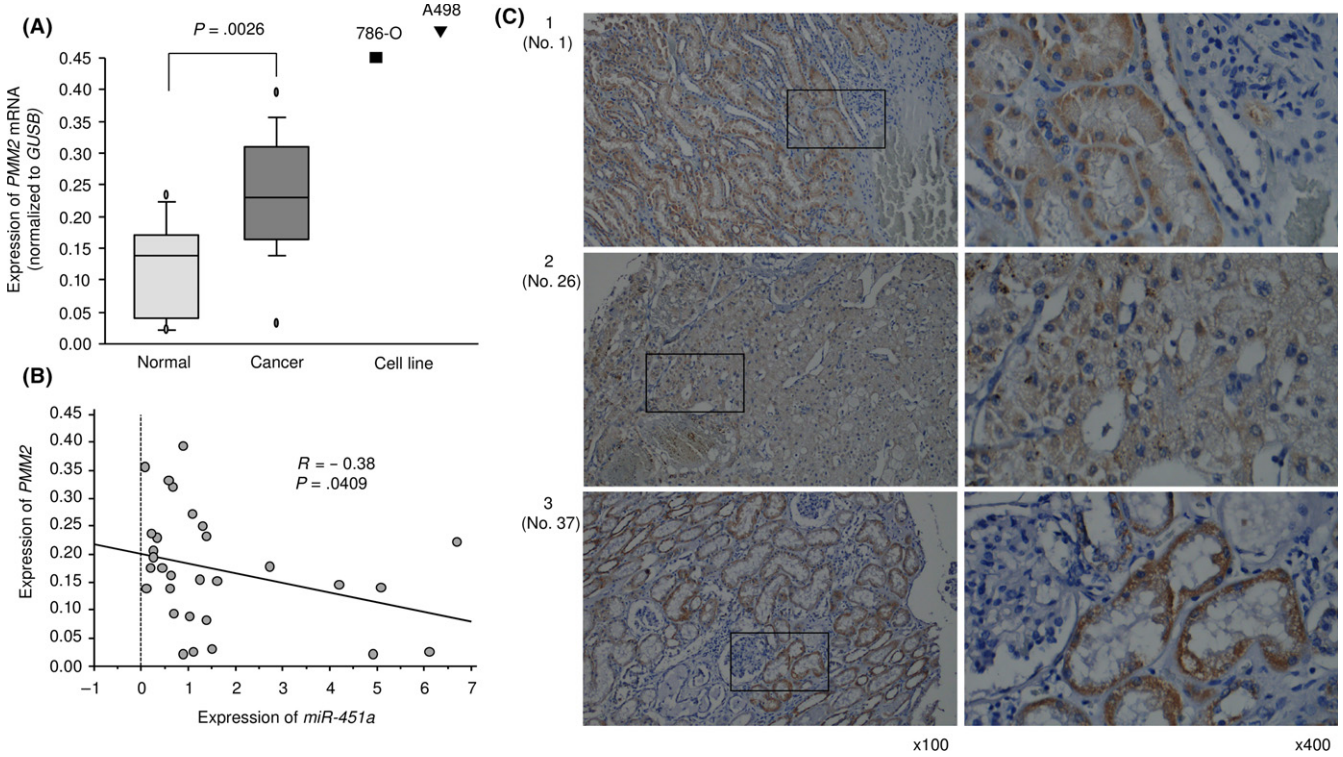

FIGURE 6 Expression of *PMM2* in clinical specimens of renal cell carcinoma. A, Expression levels of *PMM2* in renal cell carcinoma clinical specimens. *GUSB* was used as an internal control. B, A negative correlation between *PMM2* expression and *miR-451a* ($R = -.38$ and $P = .0409$). Spearman's rank test was used to evaluate the correlation. C, Immunostaining showed that phosphomannomutase 2 (PMM2) was strongly expressed in several cancer lesions (magnification, ×100 [left panels] and ×400 [right panels])

3.9 | Clinical significance of *PMM2* in RCC pathogenesis using TCGA database

To investigate the clinical significance of *PMM2* in RCC pathogenesis, we asked whether the *PMM2* expression level affected disease-free survival (DFS) in RCC. We found that high expression levels of *PMM2* were significantly associated with low DFS in RCC patients ($P < .0001$; Figure 9A). Furthermore, we analyzed the relationships among *PMM2* expression levels and tumor T stage, lymph node metastasis, disease stage, and histologic grade in RCC. *PMM2* expression levels were significantly higher in the more advanced tumor stages and histologic grades (Figure 9B-E).

Additionally, we undertook univariable and multivariable Cox hazard regression analyses to investigate the clinical significance of *PMM2* expression along with other clinical factors in the overall survival of RCC patients. Multivariate analysis showed that high *PMM2* expression and tumor stage were independent predictive factors for overall survival (hazard ratio = 1.26, $P = .0487$ and hazard ratio = 0.76, $P = .0353$, respectively; Table 4). These results suggested that *PMM2* may be closely associated with tumor progression and malignancy in RCC.

4 | DISCUSSION

The aberrant expression of miRNAs disrupts regulated RNA networks in various type of cancer cells and therefore contributes substantially to the pathogenesis of human cancer.[30] Therefore, understanding miRNA signatures is essential to clarifying their roles in the pathology of human cancer cells. We previously characterized several miRNAs that had significant antitumor functions in RCC cells. For example, *miR-101* was significantly reduced in RCC tissues and the restoration of *miR-101* inhibited RCC aggressiveness through targeting the *UHRF1* gene.[9] More recently, we showed that *miR-10a-5p* was downregulated in primary and tyrosine-kinase inhibitor-treated RCC specimens and directly regulated the *SKA1* gene. *SKA1* was overexpressed and knockdown of *SKA1* inhibited migration and invasion of RCC cells.[22]

Our present data showed that expression of *miR-451a* was significantly reduced in primary RCC. Furthermore, ectopic expression of *miR-451a* resulted in inhibition of cancer cell migratory and invasive abilities in RCC, indicating that *miR-451a* functions as a tumor suppressor in RCC. Previous reports showed that expression of *miR-451* was downregulated in several types of human cancers. In bladder cancer, *miR-451* expression was significantly reduced in cancer tissues compared with adjacent tissues and that restoration of *miR-451* reduced cancer cell migration and invasive abilities.[31,32] Furthermore, low expression of *miR-451* was associated with advanced tumor stage and high pathological grade in bladder cancer.[32] Our previous data showed that *miR-451a* acted as an antitumor miRNA through targeting *ESDN*/*DCBLD2* in head and neck squamous cell carcinoma.[12]

In this study, we identified 16 putative oncogenic targets by *miR-451a* regulation in RCC cells. Interestingly, among these targets,

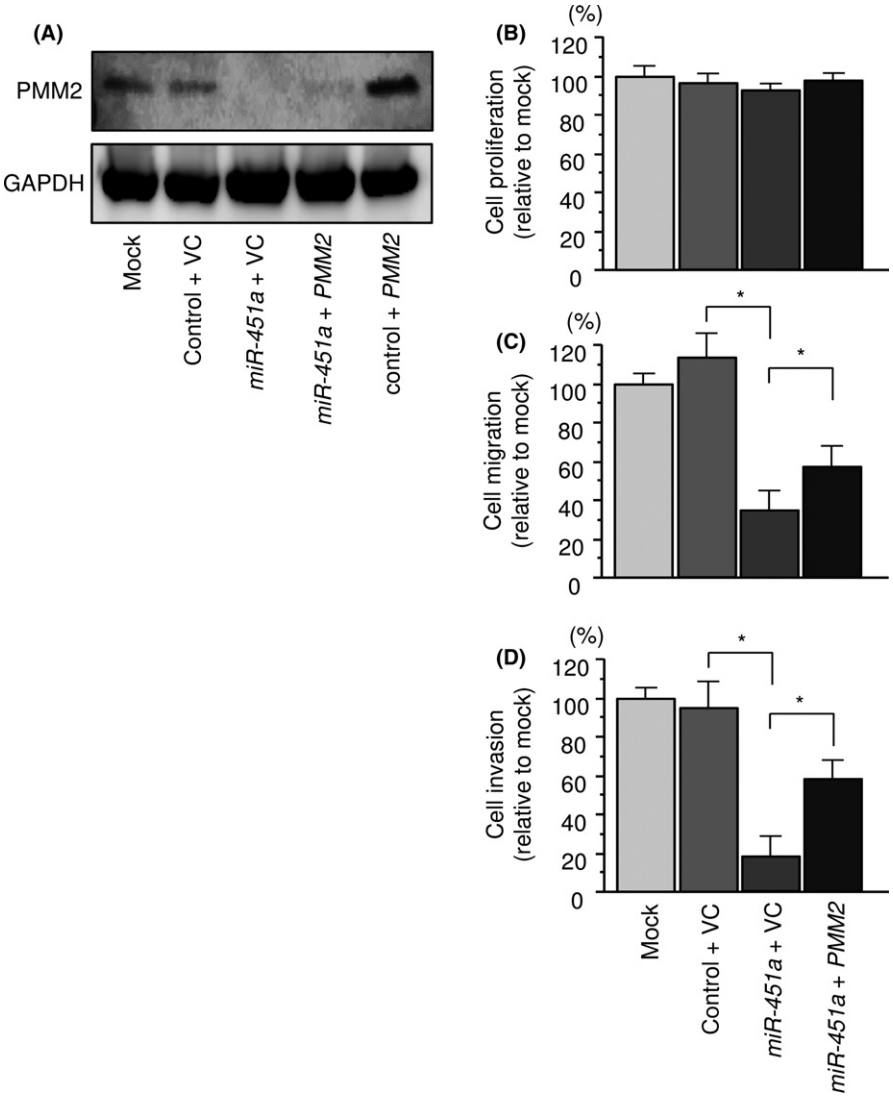

FIGURE 7 Effects of co-transfection of *PMM2*/*miR-451a* in 786-O renal cell carcinoma cells. A, Phosphomannomutase 2 (PMM2) protein expression was evaluated by Western blot analysis of 786-O cells 72 hours after reverse transfection with *miR-451a* and 48 hours after forward transfection with the *PMM2* vector. GAPDH was used as a loading control. B, Cell proliferation was determined using XTT assays 72 hours after reverse transfection with *miR-451a* and 48 hours after forward transfection with the *PMM2* vector. C, Cell migration activity was assessed by wound healing assays 48 hours after reverse transfection with *miR-451a* and 24 hours after forward transfection with the *PMM2* vector. D, Cell invasive activity was characterized by invasion assays 48 hours after reverse transfection with *miR-451a* and 24 h after forward transfection with *PMM2* vector. *$P < .0001$. VC, Vector Control

expression of 9 genes (*PMM2*, *CRELD2*, *CLEC2D*, *SPC25*, *BST2*, *EVL*, *TBX15*, *DPYSL3*, and *NAMPT*) were significantly associated with poor prognosis of the patients with RCC by TCGA database analyses. These targets might be potential therapeutic targets for RCC and the search for RNA networks controlled by antitumor *miR-451a* and its targets are important for elucidation of the pathogenesis of RCC. In the present study, we identified *PMM2* as an oncogenic gene in RCC cells. Moreover, overexpressed *PMM2* was involved RCC pathogenesis. *PMM2* codes for an enzyme that converts mannose-6-phosphate to mannose-1-phosphate and participates in a metabolic pathway in glycan synthesis.[33-35] Protein glycosylation is an important contributor to cancer progression, including cell growth, tumor-induced immunomodulation, and eventual metastasis.[36] Previous reports indicated that cancer cells, including RCC, are characterized by an aberrant increase in protein N-glycosylation.[37,38] In clear cell RCC, upregulation of protein glycosylation in cancer cells may be useful in diagnosis and determining disease prognosis.[39] Furthermore, N-glycosylation is involved in cell adhesion and is associated with reduced expression of E-cadherin, which modulates the metastatic potential of cancer cells.[37,40] We hypothesize that this pathway might contribute to cancer pathogenesis such that upregulation of *PMM2* might enhance cancer cell aggressiveness by increased N-glycosylation. In support of this hypothesis, TCGA database showed that high expression of *PMM2* was associated with poor prognosis even in other types of cancer, for example, bladder cancer, breast cancer, head and neck squamous cell carcinoma, glioma, and melanoma (Figure S2).

Interestingly, a previous report showed that *miR-451* was controlled by glucose levels and regulated cancer aggressiveness through the AMP-activated protein kinase pathway and mTOR activation in glioblastoma.[15] Thus, *miR-451* regulated pathways may be involved in glucose-related metabolic pathways and regulate cancer aggressiveness. Further research into *miR-451*/*PMM2*-modulated pathways in cancer will be necessary. To investigate *PMM2*-mediated pathways in RCC, we undertook genome-wide gene expression analyses using *PMM2* knockdown cells. We identified 27 genes that were regulated by *PMM2* in RCC. Among them, the expression of 10 genes was elevated (*CD7*, *CCNE2*, *ASB2*, *RCN3*,

TABLE 3 Candidate downstream genes modulated by *PMM2* in renal cell carcinoma cells

Gene symbol	Gene name	GEO expression data fold-change (tumor/normal)	Log_2 (si-*PMM2*_1/mock)	Log_2 (si-*PMM2*_2/mock)	Average Log_2 (si-*PMM2*/mock)	Cytoband	TCGA data OS (*P*-value)
GNLY	Granulysin	5.987	−2.465	−2.548	−2.506	hs|2p11.2	.09360000
TTF2	Transcription termination factor, RNA polymerase II	1.312	−3.407	−1.139	−2.273	hs|1p13.1	.27800000
CD7	CD7 molecule	1.981	−1.935	−2.522	−2.228	hs|17q25.3	.00001220
CCNE2	Cyclin E2	2.430	−3.101	−1.251	−2.176	hs|8q22.1	.00664000
NLGN1	Neuroligin 1	2.422	−1.377	−2.500	−1.938	hs|3q26.31	.03910000*
TMEM184B	Transmembrane protein 184B	1.525	−1.128	−2.639	−1.883	hs|22q13.1	.96300000
ASB2	Ankyrin repeat and SOCS box containing 2	1.804	−2.534	−1.194	−1.864	hs|14q32.12	.01680000
ASPH	Aspartate β-hydroxylase	1.727	−1.414	−2.244	−1.829	hs|8q12.3	.22000000
MAML3	Mastermind-like 3 (Drosophila)	1.364	−1.644	−1.923	−1.784	hs|4q31.1	.00010700*
RCN3	Reticulocalbin 3, EF-hand calcium binding domain	1.314	−2.325	−1.103	−1.714	hs|19q13.33	.00000636
CAMK1	Calcium/calmodulin-dependent protein kinase I	1.324	−1.566	−1.471	−1.519	hs|3p25.3	.54600000
P2RX7	Purinergic receptor P2X, ligand gated ion channel, 7	8.047	−1.746	−1.134	−1.440	hs|12q24.31	.95700000
KDM1B	Lysine (K)-specific demethylase 1B	1.342	−1.291	−1.544	−1.417	hs|6p22.3	.00939000*
OAS3	2′-5′-oligoadenylate synthetase 3, 100kda	2.919	−1.490	−1.287	−1.388	hs|12q24.13	.97300000
HSF1	Heat shock transcription factor 1	1.324	−1.685	−1.083	−1.384	hs|8q24.3	.00126000
PMM2	Phosphomannomutase 2	1.580	−1.304	−1.376	−1.340	hs|16p13.2	.000000218

(Continues)

TABLE 3 (Continued)

Gene symbol	Gene name	GEO expression data fold-change (tumor/normal)	Log_2 (si-*PMM2*_1/mock)	Log_2 (si-*PMM2*_2/mock)	Average Log_2 (si-*PMM2*/mock)	Cytoband	TCGA data OS (*P*-value)
CDKN2B	Cyclin-dependent kinase inhibitor 2B (p15, inhibits CDK4)	3.355	−1.237	−1.434	−1.335	hs|9p21.3	.00542000*
PAQR4	Progestin and adipoq receptor family member IV	5.134	−1.567	−1.087	−1.327	hs|16p13.3	.00152000
CD37	CD37 molecule	6.272	−1.154	−1.420	−1.287	hs|19q13.33	.01880000
SOX11	SRY (sex determining region Y)-box 11	5.969	−1.334	−1.236	−1.285	hs|2p25.2	.04050000
XAF1	XIAP associated factor 1	2.349	−1.044	−1.489	−1.266	hs|17p13.1	.00001720
DEPDC1	DEP domain containing 1	2.606	−1.253	−1.197	−1.225	hs|1p31.2	.00011100
SAMHD1	SAM domain and HD domain 1	2.764	−1.225	−1.163	−1.194	hs|20q11.23	.16600000
P2RY1	Purinergic receptor p2y, g-protein coupled, 1	1.427	−1.167	−1.142	−1.155	hs|3q25.2	.00051400*
LOC100422737	Uncharacterized loc100422737	1.322	−1.093	−1.199	−1.146	hs|6q21	No data
DOCK9	Dedicator of cytokinesis 9	1.614	−1.158	−1.087	−1.123	hs|13q32.3	.00001100*
SLC39A10	Solute carrier family 39 (zinc transporter), member 10	1.331	−1.074	−1.137	−1.105	hs|2q32.3	.01820000*
RNF125	Ring finger protein 125, e3 ubiquitin protein ligase	1.526	−1.060	−1.060	−1.060	hs|18q12.1	.03820000*

GEO, Gene Expression Omnibus; OS, overall survival; TCGA, The Cancer Genome Atlas.

*, poor prognosis with low expression.

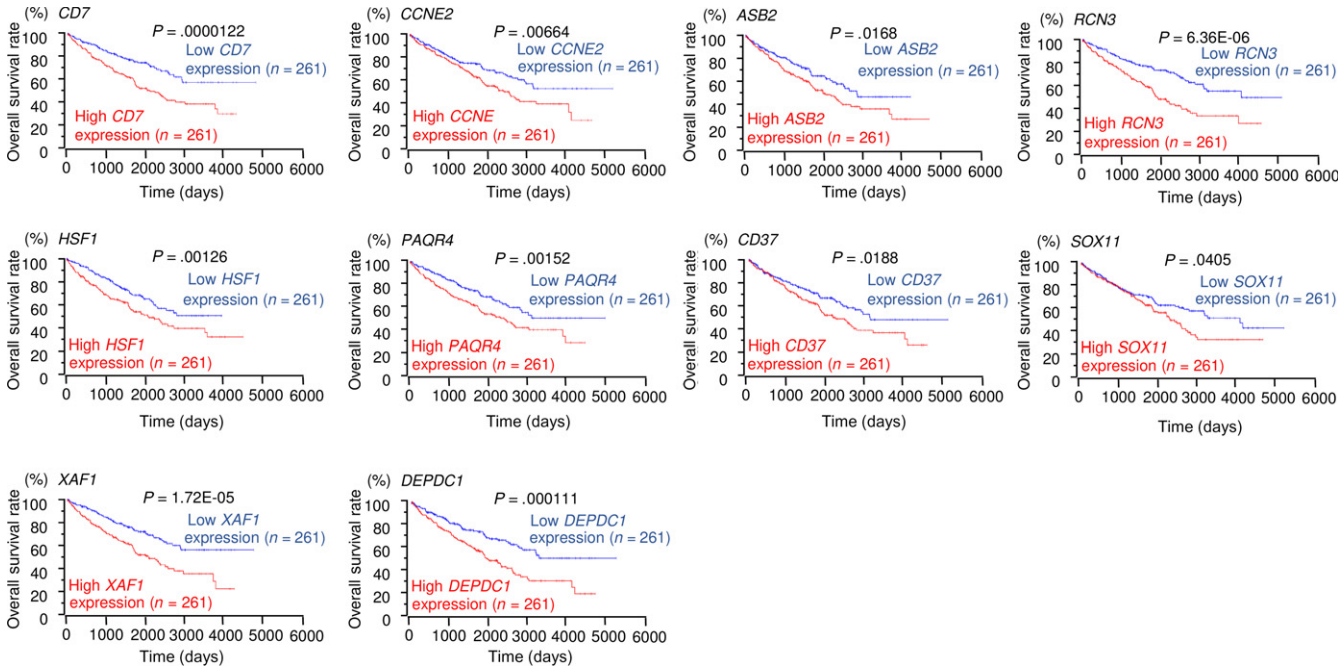

FIGURE 8 The Cancer Genome Atlas database analysis of *PMM2*-mediated downstream genes in renal cell carcinoma. Kaplan-Meier curves of 10 genes whose high expression levels were associated with poor prognosis in renal cell carcinoma

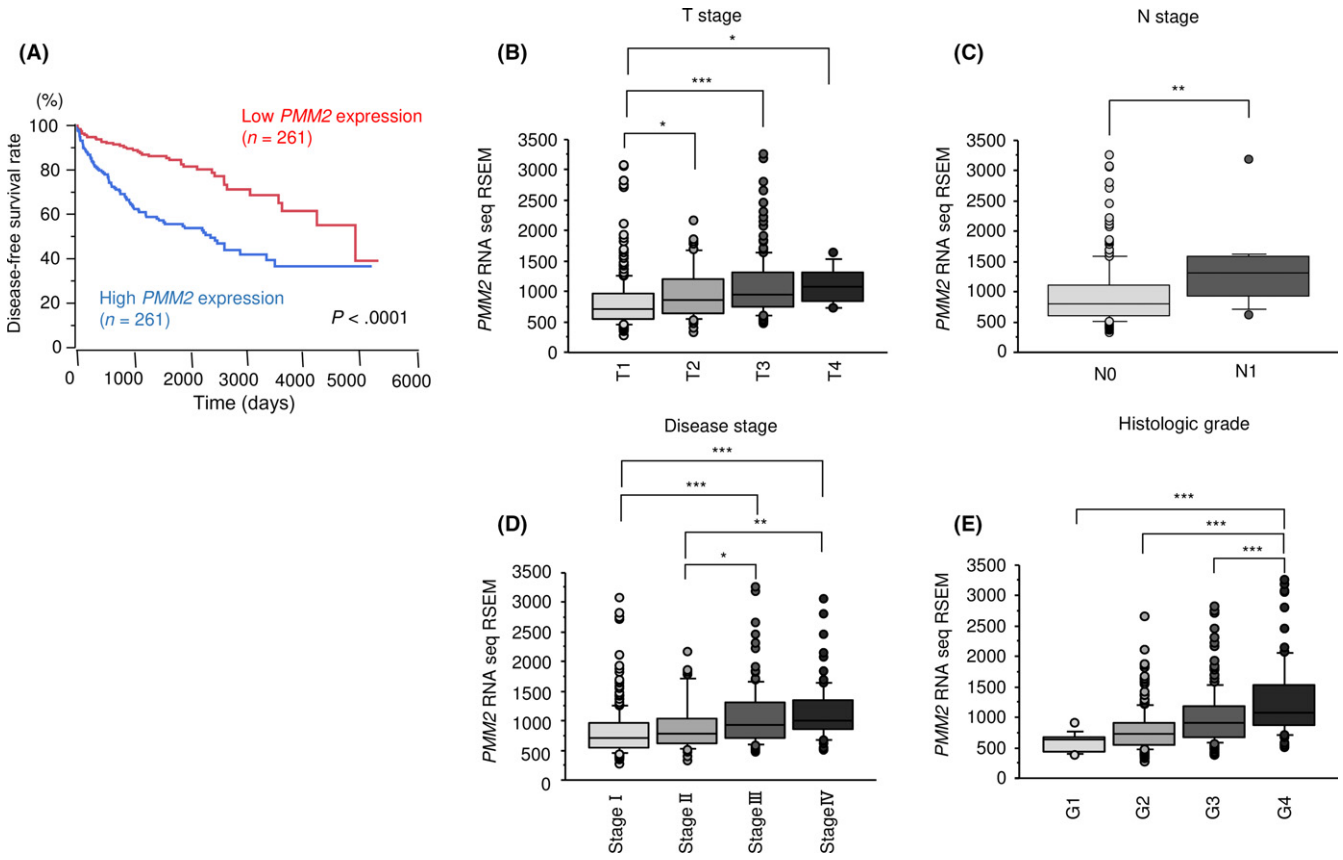

FIGURE 9 Kaplan-Meier curves for disease-free survival based on *PMM2* expression in patients with renal cell carcinoma, and expression levels of *PMM2* according to T stage, N stage, tumor stage, and histologic grade. All patients' data were obtained from The Cancer Genome Atlas database. A, Kaplan-Meier survival curves for disease-free survival based on *PMM2* expression in patients with renal cell carcinoma. B-E, Relationships between expression levels of *PMM2* and T stage, N stage, disease stage, and histologic grade. *$P < .05$, **$P < .005$, ***$P < .0001$

TABLE 4 Univariable and multivariable Cox hazard regression models for overall survival in renal cell carcinoma

		Univariable			Multivariable		
Variable	Group	HR	95% CI	*P*-value	HR	95% CI	*P*-value
PMM2 expression	High/low	1.35	1.10-1.68	.0047	1.26	1.002-1.58	.0487
Age, years	<60/≥60	0.78	0.64-0.97	.0265	0.82	0.66-1.01	.0703
Gender	Male/female	1.13	0.90-1.41	.279	-	-	-
Stage	I+II/III+IV	0.67	0.52-0.84	.0007	0.76	0.59-0.98	.0353
Histologic grade	G1+2/G3+4	0.68	0.55-0.85	.0006	0.81	0.64-1.03	.0896
Lymph node metastasis	Positive/negative	1.25	0.44-2.74	.648	-	-	-

-, Not analyzed in multivariate analysis; CI, confidence interval; HR, hazard ratio.

HSF1, *PAQR4*, *CD37*, *SOX11*, *XAF1*, and *DEPDC1*) and their expression levels were significantly associated with poor prognosis in RCC patients according to TCGA database ($P < .05$). Elucidation of novel *PMM2*-mediated pathways may improve our understanding of RCC aggressiveness.

In conclusion, our data revealed that expression of *miR-451a* was significantly downregulated in clinical RCC cells. Moreover, *miR-451a* acted as a tumor suppressor through the targeting of *PMM2*. Phosphomannomutase 2 was strongly expressed in RCC cells and its silencing significantly inhibited cancer cell migration and invasive abilities. In clinical analysis, high expression of *PMM2* was significantly associated with shorter DFS and lower survival rates. In short, *PMM2*-regulated genes are deeply involved in RCC pathogenesis. Elucidation of the pathways mediated by the *miR-451a*/*PMM2* axis should improve our understanding of oncogenic mechanisms and lead to new treatment strategies in RCC.

ACKNOWLEDGMENTS

The present study was supported by the Japan Society for the Promotion of Science (KAKENHI grant nos. 16K20125, 17K11160, 16H05462, and 15K10801).

CONFLICT OF INTEREST

The authors have no conflict of interest.

ORCID

Yasutaka Yamada http://orcid.org/0000-0002-0070-1590
Takayuki Arai http://orcid.org/0000-0002-3888-9576

REFERENCES

1. Capitanio U, Montorsi F. Renal cancer. *Lancet*. 2016;387:894-906.
2. Figlin R, Sternberg C, Wood CG. Novel agents and approaches for advanced renal cell carcinoma. *J Urol*. 2012;188:707-715.
3. Gupta K, Miller JD, Li JZ, Russell MW, Charbonneau C. Epidemiologic and socioeconomic burden of metastatic renal cell carcinoma (mRCC): a literature review. *Cancer Treat Rev*. 2008;34:193-205.
4. Goto Y, Kurozumi A, Enokida H, Ichikawa T, Seki N. Functional significance of aberrantly expressed microRNAs in prostate cancer. *Int J Urol*. 2015;22:242-252.
5. Bartel DP. MicroRNAs: genomics, biogenesis, mechanism, and function. *Cell*. 2004;116:281-297.
6. Friedman RC, Farh KK, Burge CB, Bartel DP. Most mammalian mRNAs are conserved targets of microRNAs. *Genome Res*. 2009;19:92-105.
7. Koshizuka K, Hanazawa T, Fukumoto I, Kikkawa N, Okamoto Y, Seki N. The microRNA signatures: aberrantly expressed microRNAs in head and neck squamous cell carcinoma. *J Hum Genet*. 2017;62:3-13.
8. Kurozumi A, Goto Y, Okato A, Ichikawa T, Seki N. Aberrantly expressed microRNAs in bladder cancer and renal cell carcinoma. *J Hum Genet*. 2017;62:49-56.
9. Goto Y, Kurozumi A, Nohata N, et al. The microRNA signature of patients with sunitinib failure: regulation of UHRF1 pathways by microRNA-101 in renal cell carcinoma. *Oncotarget*. 2016;7:59070-59086.
10. Goto Y, Kojima S, Nishikawa R, et al. MicroRNA expression signature of castration-resistant prostate cancer: the microRNA-221/222 cluster functions as a tumour suppressor and disease progression marker. *Br J Cancer*. 2015;113:1055-1065.
11. Koshizuka K, Nohata N, Hanazawa T, et al. Deep sequencing-based microRNA expression signatures in head and neck squamous cell carcinoma: dual strands of pre-miR-150 as antitumor miRNAs. *Oncotarget*. 2017;8:30288-30304.
12. Fukumoto I, Kinoshita T, Hanazawa T, et al. Identification of tumour suppressive microRNA-451a in hypopharyngeal squamous cell carcinoma based on microRNA expression signature. *Br J Cancer*. 2014;111:386-394.
13. Pan X, Wang R, Wang ZX. The potential role of miR-451 in cancer diagnosis, prognosis, and therapy. *Mol Cancer Ther*. 2013;12:1153-1162.
14. Minna E, Romeo P, Dugo M, et al. miR-451a is underexpressed and targets AKT/mTOR pathway in papillary thyroid carcinoma. *Oncotarget*. 2016;7:12731-12747.
15. Godlewski J, Bronisz A, Nowicki MO, Chiocca EA, Lawler S. microRNA-451: a conditional switch controlling glioma cell proliferation and migration. *Cell Cycle*. 2010;9:2742-2748.
16. Liu Z, Miao T, Feng T, et al. miR-451a inhibited cell proliferation and enhanced tamoxifen sensitive in breast cancer via macrophage migration inhibitory factor. *Biomed Res Int*. 2015;2015:207684.
17. Gao Z, Liu R, Liao J, et al. Possible tumor suppressive role of the miR-144/451 cluster in esophageal carcinoma as determined by principal component regression analysis. *Mol Med Rep*. 2016;14:3805-3813.
18. Zhang F, Huang W, Sheng M, Liu T. MiR-451 inhibits cell growth and invasion by targeting CXCL16 and is associated with prognosis of osteosarcoma patients. *Tumour Biol*. 2015;36:2041-2048.

19. Tang Y, Wan W, Wang L, Ji S, Zhang J. microRNA-451 inhibited cell proliferation, migration and invasion through regulation of MIF in renal cell carcinoma. *Int J Clin Exp Pathol*. 2015;8:15611-15621.
20. Okato A, Arai T, Kojima S, et al. Dual strands of pre-miR150 (miR1505p and miR1503p) act as antitumor miRNAs targeting SPOCK1 in naive and castration-resistant prostate cancer. *Int J Oncol*. 2017;51:245-256.
21. Yamada Y, Koshizuka K, Hanazawa T, et al. Passenger strand of miR-145-3p acts as a tumor-suppressor by targeting MYO1B in head and neck squamous cell carcinoma. *Int J Oncol*. 2018;52:166-178.
22. Arai T, Okato A, Kojima S, et al. Regulation of spindle and kinetochore-associated protein 1 by antitumor miR-10a-5p in renal cell carcinoma. *Cancer Sci*. 2017;108:2088-2101.
23. Yamada Y, Nishikawa R, Kato M, et al. Regulation of HMGB3 by antitumor miR-205-5p inhibits cancer cell aggressiveness and is involved in prostate cancer pathogenesis. *J Hum Genet*. 2018;63:195-205.
24. Koshizuka K, Hanazawa T, Kikkawa N, et al. Regulation of ITGA3 by the anti-tumor miR-199 family inhibits cancer cell migration and invasion in head and neck cancer. *Cancer Sci*. 2017;108:1681-1692.
25. Nishikawa R, Goto Y, Sakamoto S, et al. Tumor-suppressive microRNA-218 inhibits cancer cell migration and invasion via targeting of LASP1 in prostate cancer. *Cancer Sci*. 2014;105:802-811.
26. Kurozumi A, Goto Y, Matsushita R, et al. Tumor-suppressive microRNA-223 inhibits cancer cell migration and invasion by targeting ITGA3/ITGB1 signaling in prostate cancer. *Cancer Sci*. 2016;107:84-94.
27. OncoLnc JA. Linking TCGA survival data to mRNAs, miRNAs, and lncRNAs. *PeerJ Comput Sci*. 2016;2:e67.
28. Gao J, Aksoy BA, Dogrusoz U, et al. Integrative analysis of complex cancer genomics and clinical profiles using the cBioPortal. *Sci Signal*. 2013;6:pl1.
29. Cerami E, Gao J, Dogrusoz U, et al. The cBio cancer genomics portal: an open platform for exploring multidimensional cancer genomics data. *Cancer Discov*. 2012;2:401-404.
30. Esquela-Kerscher A, Slack FJ. Oncomirs - microRNAs with a role in cancer. *Nat Rev Cancer*. 2006;6:259-269.
31. Wang J, Zhao X, Shi J, et al. miR-451 suppresses bladder cancer cell migration and invasion via directly targeting c-Myc. *Oncol Rep*. 2016;36:2049-2058.
32. Zeng T, Peng L, Chao C, et al. miR-451 inhibits invasion and proliferation of bladder cancer by regulating EMT. *Int J Clin Exp Pathol*. 2014;7:7653-7662.
33. Freeze HH. Towards a therapy for phosphomannomutase 2 deficiency, the defect in CDG-Ia patients. *Biochem Biophys Acta*. 2009;1792:835-840.
34. Schiff M, Roda C, Monin ML, et al. Clinical, laboratory and molecular findings and long-term follow-up data in 96 French patients with PMM2-CDG (phosphomannomutase 2-congenital disorder of glycosylation) and review of the literature. *J Med Genet*. 2017;54:843-851.
35. Chan B, Clasquin M, Smolen GA, et al. A mouse model of a human congenital disorder of glycosylation caused by loss of PMM2. *Hum Mol Genet*. 2016;25:2182-2193.
36. Stowell SR, Ju T, Cummings RD. Protein glycosylation in cancer. *Annu Rev Pathol*. 2015;10:473-510.
37. Borzym-Kluczyk M, Radziejewska I, Cechowska-Pasko M, Darewicz B. Reduced expression of E-cadherin and increased sialylation level in clear cell renal cell carcinoma. *Acta Biochim Pol*. 2017;64:465-470.
38. Dennis JW, Granovsky M, Warren CE. Protein glycosylation in development and disease. *BioEssays*. 1999;21:412-421.
39. Gbormittah FO, Bones J, Hincapie M, Tousi F, Hancock WS, Iliopoulos O. Clusterin glycopeptide variant characterization reveals significant site-specific glycan changes in the plasma of clear cell renal cell carcinoma. *J Proteome Res*. 2015;14:2425-2436.
40. Hsiao CT, Cheng HW, Huang CM, et al. Fibronectin in cell adhesion and migration via N-glycosylation. *Oncotarget*. 2017;8:70653-70668.

SUPPORTING INFORMATION

Additional Supporting Information may be found online in the supporting information tab for this article.

How to cite this article: Yamada Y, Arai T, Sugawara S, et al. Impact of novel oncogenic pathways regulated by antitumor *miR-451a* in renal cell carcinoma. *Cancer Sci*. 2018;109:1239–1253. https://doi.org/10.1111/cas.13526